Synthesis of Isophthalic Acid-Carbazole Coordination Poly-mers with Stackingdependent Ultralong Room Temperature Phosphorous and White-Light Emission

Hong-Ru Fu *, Hong Chen, Kun Zhang, Ting Li, Xue-Li Zhu *

Posted Date: 27 April 2023

doi: 10.20944/preprints202304.1017.v1

Keywords: coordination polymers; room temperature phosphorescence; multicolor emission

Article

Synthesis of Isophthalic Acid-Carbazole Coordination Polymers with Stacking-Dependent Ultralong Room Temperature Phosphorescence and White-Light Emission

Hong-Ru Fu [1,*], Hong Chen [1,2] and Kun Zhang [1],Ting Li [1] and Xue-Li Zhu [1,*]

[1] College of Chemistry and Chemical Engineering Luoyang Normal University, Luoyang 471934, P. R. China. E-mail: hongrufu2015@163.com, zhuxueli@hnu.edu.cn

[2] Luoyang Key Laboratory of Organic Functional Molecules, College of Food and Drug, Luoyang Normal University, Luoyang, 471934, P. R. China

* Correspondence: hongrufu2015@163.com (H.-R.F.); zhuxueli@hnu.edu.cn (X.-L.Z.)

† Materials, crystallographic and photoluminescence studies. CCDC 2219861, 2219862, 2219863. For ESI and crystallographic data in CIF or other electronic format see https://doi.org/10.1039/d2sc03729g.

Abstract: Exploiting the relationship between the stacking modes of molecules and room-temperature phosphorescence (RTP) performance is of great important to design afterglow materials. A series of coordination polymers [Cd(CzIP)] (1), [Cd(CzIP)(DMI)] (DMI = 1,3-Dimethyl-2-imidazolidinone) (2) and [$Cd_2(CzIP)_2(H_2O)_2$] (3) base on carbazole–isophthalic acid are synthesized via a solvothermal method. These compounds exhibit stacking-dependent RTP. Compounds 1 and 2 exhibit obvious time-dependent RTP with the afterglow color from orange to green, and show white-light emission owing to fluorescence and phosphorescence dual emission. Compound 3 featuring the strong π–π stacking showed the weak phosphorescence with the short lifetime. It reveals that the phosphorescence efficiency is not proportional to the overlap of π-π stacking, the triplet excited states of discrete dimer mode rather than H-aggregation can dominate the generation of room-temperature phosphorescence. These results indicate that coordination induction is an efficient approach to regulate the aggregation of chromophores, further modulate the room-temperature phosphorescence.

Keywords: dynamic room temperature phosphorescence; coordination polymers; aggregate states

1. Introduction

Persistent room temperature phosphorescence with the unique photophysical properties (e.g., triplet-state harvesting, long lifetime and temperature sensitivity) are drawing considerable attention in many fields, such as bioimaging, anticounterfeiting and light emitting diodes, and so on.[1-7] In view of the traditional noble meta-based phosphorescent materials exists the problem of instability in air, high cost and complicated synthesis, more and more new material systems are being developed based on the principles of host–guest system, crystallization and polymer matrix embedding.[8-12]

Today, white-light emitting materials are playing an important role in solid-state lighting and modern display.[13] Till now, the common method for white-light emission is to cooperate multiple emitters to meet the RGB colors. In comparison with multicomponent sources, white-light emitted directly from single-phased materials is much more attractive, because it not only can simplify the procedure of the combined emitters, void the balance for both excitation and emission between mixed components,[14-16] but also reduce the loss of energy transfer.[17] Besides, white-light emitting materials, of particular with phosphorescence emission, owing the much higher electroluminescence efficiency, are much more desirable. However, the majority of luminophores obey Kasha's rule, it is difficulty to modulate excited states (excitation wavelength, emission lifetimes, etc) and energy transfer in a single structure,[18-20] obtaining the room temperature phosphorescent materials, especially white-light emitters, is also a great challenge.

The photophysical behaviors of luminescent materials depend largely on aggregation forms and the configuration of chromophores.[21] Enlightened by this, we focus on the crystal engineering of coordination polymers to exploit materials with multi-emission including RTP and white-light emission. Coordination polymers as a class of crystalline materials were constructed via coordination interactions between metal ions and organic ligands.[22] The rigidity of organic ligands containing chromophores can be significantly enhanced by the coordination bonds with metal ions.[23,24] Meanwhile, the highly ordered arrangement of the chromophores could be achieved, which are beneficial for obtaining the highly efficient luminescence.[25] Importantly, coordination polymers provide a smart platform to tune flexibly the packing and conformation of chromophores. Compared the crystallization of pure organics of isomerization, through the scaffold of coordination polymers, it is in favor of generating the discrete stack rather than compact structure, eliminating the fluorescence quenching caused by strong π–π interaction, instead, achieving the monomer, dimer, even excimer emission.[26-31] Beyond that, the diversified arrangement and configuration of chromophores could be integrated in one compound, the compound could show the multiple mission, providing great opportunities for white light generation. Recently, some coordination polymers have been prepared, and the excellent room temperature phosphorescence was exhibited. For examples, were deliberately synthesized, three coordination polymers were synthesized based on Himpc [5-(1H-1,2,4-imidazol-1-yl)nicotinic acid] phosphor via a solvothermal method, and these compounds showed time-resolved color-changing afterglow phosphorescence performances.[32] Pan's group reported that a series of metal-organic coordination polymers displaying color-tunable long persistent luminescence (LPL) were synthesized by the selfassembly of HTzPTpy ligand with different cadmium halides (X = Cl, Br, and I).[33] These results demonstrate that coordination polymers can act as a good substrate to regulate the room temperature phosphorescence.

Carbazole has been as a triplet sensitizer (superior building block) in long-lived luminescence systems, it has been demonstrated by a series of organic room temperature phosphorescence molecules.[34-36] Here, isophthalate was decorated on carbazole, a molecule 5-(carbazol-9-yl) isophthalate (CzIP) with coordination nodes was synthesized. Interestingly, isophthalate could act as an intersystem crossing (ISC) facilitator, resulting in CzIP exhibits the afterglow emission at room temperature. Through the coordination assemblies of metal nodes and CzIP, three coordination polymers crystals [Cd(CzIP)] (1), [Cd(CzIP)(DMI)] (DMI = 1,3-Dimethyl-2-imidazolidinone) (2) and [Cd_2(CzIP)$_2$(H_2O)$_2$] (3) were synthesized. These compounds all exhibit fluorescence and phosphorescence dual emission, the emission behaviors could be tuned via the regulation of the coordination microenvironment. It found that the phosphorescence efficiency is not directly proportional to the overlap of parallel carbazole dimer in the vertical orientation, instead, the excessively serious overlap can prompt the generation of the intramolecular excimer emission and weaken the phosphorescence emission. Meanwhile, the white-light emission could be achieved in these compounds with single wavelength excitation. These results not only provide a method to tune the arrangement of the chromophores to obtain fluorescence and phosphorescence dual-emitting materials, but also demonstrate a promising strategy to design single-phased white-light materials.

2. Results and discussion

2.1. Materials and Methods.

All chemical materials were obtained from commercial sources and used without further purification. 5-(carbazol-9-yl) isophthalate (CzIP) was synthesized by following the published method.[37] Powder X-ray diffraction (PXRD) patterns were acquired on a Bruker D8 ADVANCE diffractometer with Cu Kα (λ = 1.5418 Å) radiation in the range of 2θ = 5–50° with a step size of 0.025º and an acquisition time of 2.5 s per step at room temperature. Thermogravimetric analysis (TGA) was performed on a PerkinElmer TG-7 analyzer heated from room temperature to 750 °C at a ramp rate of 5 °C/min under air atmosphere. Elemental analyses (C, H, and N) were conducted on a PerkinElmer 240C elemental analyzer. The solid state Ultraviolet-visible (UV-Vis) absorption spectrum were collected on a PerkinElmer Lambda 35 spectrophotometer under ambient conditions.

 doi:10.20944/preprints202304.1017.v1

The fluorescence spectra of CzIP in different solution with different concentrations were measured using F-4600 fluorescence spectrophotometer. The delayed (temperature-dependent) emission spectra, lifetime, time-resolved emission spectra and temperature-dependent phosphorescence spectra and quantum yields were measured on Edinburgh FLS1000 fluorescence spectrometer, and luminescence lifetimes were obtained on a single photon counting spectrometer with micro-second pulse lamp, the lifetimes of the luminescence were obtained by fitting the decay curve with a multi-exponential decay function.

2.2. Synthesis of Compounds

Compound 1: A mixture of CzIP (15 mg, 0.065 mmol), D-cyclopentylglycine (15 mg, 0.10 mmol) and $Zn(NO_3)_2{\cdot}6H_2O$ (60 mg, 0.20 mmol) were dissolved in H_2O and DMI (DMI = 1,3-Dimethyl-2-imidazolidinone) (8 and 2 mL), the mixture were sealed in a Teflon-lined stainless steel container and heated at 150 °C for 3 days, and then cooled to room temperature. Colorless prismatic crystals were obtained and collected by filtration. Anal. calcd (%) for $C_{20}H_{11}NO_4Zn$: C 60.80, H 2.79, N 3.55. Found (%): C 60.41, H 2.81, N 3.50.

Compound 2: CzIP (15 mg, 0.065 mmol), D-cyclopentylglycine (15 mg, 0.10 mmol) and $Cd(SO_4)_2{\cdot}8H_2O$ (50 mg, 0.06 mmol) were dissolved in H_2O and DMI (DMI = 1,3-Dimethyl-2-imidazolidinone) (8 and 2 mL), the mixture were sealed in a Teflon-lined stainless steel container and heated at 150 °C for 3 days, and then cooled to room temperature. Colorless prismatic crystals were obtained and collected by filtration. The crystals were washed with N,N-dimethylformamide (DMF) for three times to remove the surface impurities. Anal. calcd (%) for $C_{25}H_{21}CdN_3O_5$: C 53.97, H 3.78, N 7.55. Found (%): C 54.11, H 3.80, N 7.59.

Compound 3: CzIP (15 mg, 0.065 mmol), D-cyclopentylglycine (15 mg, 0.1 mmol) and $Cd(SO_4)_2{\cdot}8H_2O$ (50 mg, 0.06 mmol) were dissolved in H_2O and ethanol (EtOH) (8 and 2 mL), the mixture were sealed in a Teflon-lined stainless steel container and heated at 150 °C for 3 days, and then cooled to room temperature. Colorless prismatic crystals were obtained and collected by filtration. The crystals were washed with DMF for three times to remove the surface impurities. Anal. calcd (%) for $C_{40}H_{26}Cd_2N_2O_{10}$: C 52.20, H 2.83, N 3.05. Found (%): C 52.39, H 2.88, N 3.04.

2.3. X-ray Crystal Structures

The diffraction data were measured at 293 K with Rigaku supernova CCD system equipped with a confocal monochromated Mo-Kα radiation (λ = 0.71073 Å) by applying the ω-scan method. The structure was solved by a direct method and refined by full-matrix least-squares using SHELX-2014 [38] and Olex2.0. [39] Non-hydrogen atoms were refined with anisotropic thermal displacement coefficients. Hydrogen atoms belonging to the CzIP ligand were located in the difference Fourier map and included as fixed contributions riding on attached atoms with isotropic thermal displacement parameters 1.2 times those of their parent atoms. All hydrogen atoms were located on the geometrically ideal positions and refined using a riding model. CCDC 2219861–2219863 for 1-3. These data can be obtained free of charge via http://www.ccdc.cam.ac.uk/conts/retrieving.html (or from the Cambridge Crystallographic Data Centre, 12, Union Road, Cambridge CB2 1EZ, UK; fax: +441223 336033). The crystal structure parameters were listed in Table S1.

2.4. Structures and Optical properties

Single-crystal data analysis reveals that compound 1 crystallizes in a monoclinic *P*2/c space group. The asymmetric unit contains one Zn^{2+} ions, one CzIP ligand and two terminal water molecules (Figure S1). Each CzIP molecule coordinates four Zn^{2+} ions through the four oxygen atoms of two carboxylate groups via μ_4-η^1 : η^1 : η^1 form. Zn^{2+} ions connect CzIP molecule to form a two-dimensional (2D) layer, the layers further stack into a scaffold. Through carefully check the structure, the CzIP molecules only has one configuration in each layer (Figure S1c), the dihedral angle between the phenyl ring of the isophthalate and carbazole group is near 60°, and the carbazole groups stack a face-to face one-dimensional (1D) dimensional column with a centroid-centroid distance of 4.71 Å,

Preprints (www.preprints.org) | NOT PEER-REVIEWED | Posted: 27 April 2023 doi:10.20944/preprints202304.1017.v1

and the shortest distance is 3.70 Å (Figure 1a, 1c and S1). It should be noted that although the carbazole groups show the parallel alignment, there is a much larger slip with each other, the perpendicular overlap ratio is about 30.2%. Besides, the distances among carbazole fragments in adjacent layers range from 3.02 to 3.85 Å. As a results, compound 1 is a supramolecular structure through the packing of 2D layers, there exist multiple weak π–π and C-H···π interactions (Figure 1b, 1c),[31] also indicating the carbazole units present the discrete dimer stacking.

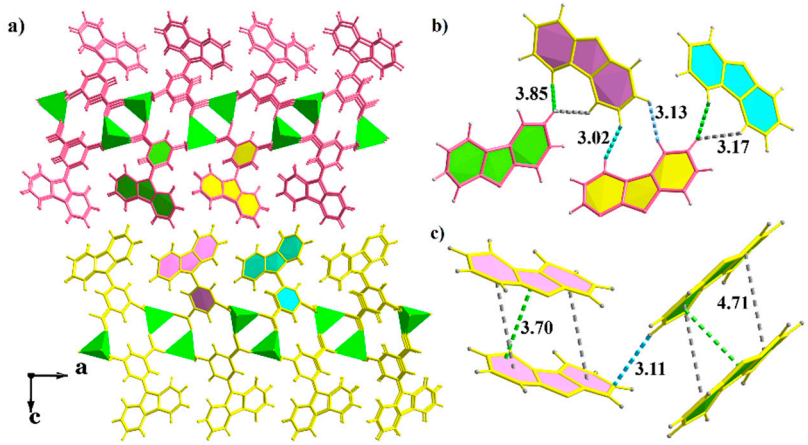

Figure 1. (a) Three-dimensional (3D) supramolecular structure of compound 1 built of two-dimensional (2D) layers through noncovalent interactions; (b) the packing of carbazole groups from the adjacent layers; (c) the distance between carbazole groups.

Compound 2 also crystallizes in a monoclinic *P*2/c space group. The asymmetric unit contains two Zn^{2+} ions, two CzIP ligand and two terminal DMI molecules (Figure S2). Each CzIP molecule coordinates four Zn^{2+} ions through the four oxygen atoms of two carboxylate groups. The isophthalates connect Zn^{2+} ions to form a layer, the carbazole chromophores as terminal units were suspended on both sides of the layer (Figure 2a). In compound 2, there is only one stack fashion of carbazoles in each layer, namely, it exhibits the head-to-tail parallel packing, like the ladder without overlap from the side view (Figure 2c), and the nearest distance is about 3.40 Å. The distance of each carbazole fragments away from the adjacent carbazole molecules is 3.0 and 3.3 Å, respectively (Figure 2b), through the calculation of MERCURY and PLATON program, there are no intramolecular and intermolecular hydrogen bonds, the interactions in compound 2 is mainly van der Waals interactions, while there are no abundant hydrogen bonds, largely suggesting that the carbazole fragments exhibit the monomer-type arrangement.

Compound 3 crystallizes in a triclinic *P*-1 space group. As shown in Figure S4, the basic unit contains two Zn^{2+} ions, Zn1 connects six oxygen atoms from one terminal water molecule and four CzIP ligands. Zn2 connects seven oxygen atoms from one terminal water molecule and four CzIP ligands. CzIP molecules have the same coordination mode, each CzIP coordinates three Zn^{2+} ions with μ_3-η^1 : η^2 : η^2 form. Compound 3 was consisted of 1D chains via supramolecular interactions. The CzIP molecules adopt twist conformations between isophthalic acid and carbazoles, as a result, the carbazole groups from the neighboring chains nearly form the face-to-face arrangement. The space of two adjacent carbazoles ranges from 3.7 to 4.5 Å between interplanar centers, and two kinds of dimeric stacking of the carbazoles exist in compound 3, such as carbazole fragments are presented with orange and yellow skeleton (Figure 3c and 3d) as well as the carbazole fragments with red and green skeleton in Figure 3e and 3f, the overlap ratio is up to approximately 62.3 and 57.4 % from the top view. The discrete dimeric stacking foreshadowed the strength of aromatic stacking interactions and presented H-aggregation. [40-43]

Preprints (www.preprints.org) | NOT PEER-REVIEWED | Posted: 27 April 2023 doi:10.20944/preprints202304.1017.v1

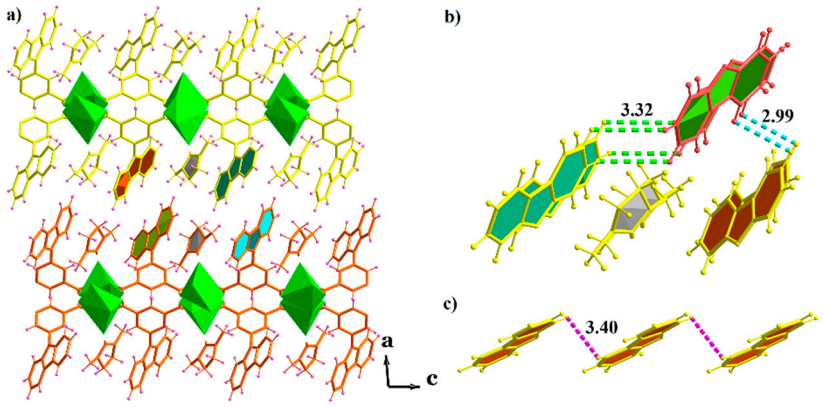

Figure 2. (a) Three-dimensional (3D) supramolecular structure built of two-dimensional (2D) layers through noncovalent interactions; (b) the packing of carbazole groups from the adjacent layers in compound 2; (c) the distance between carbazole groups.

The crystal purity and thermal stability of compounds 1-3 was investigated. The power XRD patterns of the as-synthesized crystal samples are consistent with those simulated from single-crystal data, indicating the high phase purity of the crystal samples (Figure S5-7). Meanwhile, the TGA of compounds 1-3 were carried out under air condition from 30 to 700 °C. Compound 1 showed a high stability only with a tiny weight loss of 3.9% upon heating up to 425 °C, which was attributed to the removal of the physiosorbed water and the surface solvent molecules. The further drastic weight drop suggests the decomposition of compound 1. Above 500 ºC, compound 1 experiments several exothermic processes as a consequence of the decomposition of the organic part, leading to ZnO as a final residue. The thermogravimetric analysis (TGA) showed compound 2 can maintain its framework to near 300 °C. A plateau in the TG curve from room temperature up to 300 ºC is observed. For compound 3, the weight loss was 6.23% in temperature range of 30-170 ºC, which is attributed the removel of surface water molecules and coordinated water molecules. Almost no weight loss was found for 3 until the collapse of the framework occurred at about 495 °C, the final residue is CdO powder. Totally, the weight loss behaviors of compounds 1-3 is in good line with their crystal structures. Compounds 1 and 3 exhibit the relatively compact stacking owning the stronger π–π interactions, compared to the loose packing of compound 2.

The photophysical properties of compounds 1–3 were investigated under ambient conditions. Compounds 1 and 2 are colorless crystals under natural light. Compounds 1 and 2 show the blue-white light upon 365 nm UV irradiation, interestingly, the naked-aye afterglow could be observed from compound 1 and 2 after turning off the irradiation source at ambient conditions. Especially for compound 1, the multi-color afterglow can be observed lasting about 3.5 s, and the afterglow color was changed from orange to yellow green. Unexpectedly, compounds 3 featuring the compact face-to face π–π arrangement of carbazole fragments displays the green emission, but no visible afterglow could be traced under different excitation wavelength. The prompt photoluminescence spectra of compound 1 exhibits two emission bands, with one in the blue light region and the other in the long-wavelength region ranged from 475 to 675 nm and possessing four peaks around 473, 500, 550 and 623 nm (Figure 4a). The delayed spectra of compound 1 with the delayed time 0.1 or 0.5 ms has a near perfect matching with the long-wavelength regions of the prompt spectrum, indicating that compound 1 has phosphorescence property. Compound 2 also exhibit the similar fluorescence and phosphorescence dual emission to that of compound 1, the fluorescence emission has three peaks at 375, 415 and 435 nm, the phosphorescence emission centred at about 570 and 625 nm (Figure 4b), respectively. While compound 3 emit green light with a maximum at 539 nm, the phosphorescence bands are obviously red shifted, leading to phosphorescence colors covering a large range from blue-green to orange-red. The time resolved PL spectra of compounds 1-3 were measured. The two emission bands of compound 1 at 547 and 599 nm exhibit ultralong lifetimes of 663.85 and 597.60 ms, as well as decay lifetimes of 188.34 and 50.90 ms at 570 and 610 nm for compound 2. For compound

 doi:10.20944/preprints202304.1017.v1

3, the lifetimes are 16.6 and 7.14 ms monitored at 600 and 670 nm, which is far less than the lifetimes of compounds 1 and 2 (Figure 4g-i). The phosphorescent quantum yields of compounds 1-3 are 15.73%, 11.31 and 1.65% at ambient conditions, respectively. Interestingly, based on the above results, it can find that the emission wavelength has a positive correlation with the overlap of carbazole fragments, compound 3 owing the largest overlap show the largest emission wavelength. However, no similar relationship between the overlap of carbazole fragments and the emission wavelength and afterglow lifetime of phosphorescence can be observed. It is worth mentioning that compound 3 has the compact π···π stacking between carbazole chromophores, the phosphorescence wavelengths are red-shifted progressively compared to that of compounds 1 and 2, but it did not exhibit the strong phosphorescence with the relative longer lifetime. Notably, compounds 1 and 2 showed obvious changes of color evolution from orange to green after the stopping of irradiation, especially for compound 1, indicating these two compounds exhibit the time-dependent dynamic RTP.

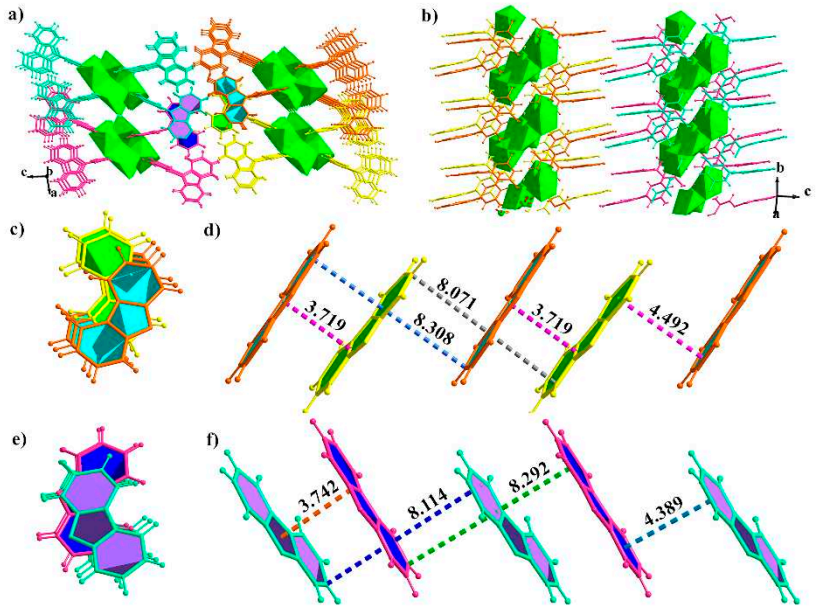

Figure 3. (a) Three-dimensional (3D) supramolecular structure of compound 3 built of one-dimensional (1D) chains through noncovalent interactions; (b) the packing of carbazole groups from the adjacent layers; (c-f) the distances between carbazole groups.

Preprints (www.preprints.org) | NOT PEER-REVIEWED | Posted: 27 April 2023 doi:10.20944/preprints202304.1017.v1

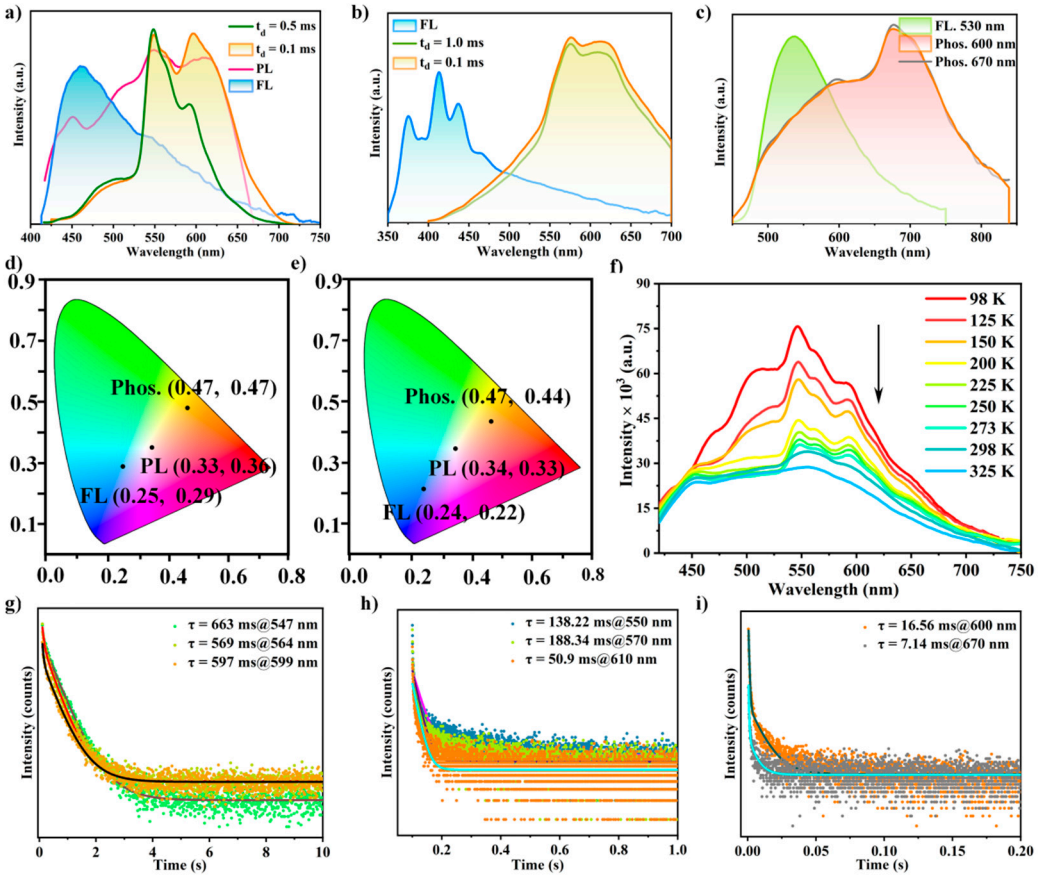

Figure 4. Photophysical properties of compounds 1-3 under ambient conditions. (a) Steady-state photoluminescence (PL), fluorescence (FL) and phosphorescence (Phos.) spectra of compound 1; (b) fluorescence and phosphorescence spectra of compound 2; (c) steady-state PL and phosphorescence spectra of compound 3; (d) corresponding CIE coordinates for fluorescence, phosphorescence and photoluminescence (PL) of compound 1; (e) corresponding CIE coordinates for FL and Phos. of compound 2; (f) normalized PL spectra of compound 1 from 98 to 350 K without door gated instrument; (g) lifetime decay profiles of the of compound 1 at 547, 564 and 599 nm; (h) lifetime decay profiles of the of compound 2 at 555, 570 and 610 nm; (i) lifetime decay profiles of the of compound 3 at 600 and 670 nm, respectively.

Besides, the photoluminescent Commission International Ed'Eclairage (CIE) coordinates of compounds 1 and 2 were (0.33, 0.36) and (0.34, 0.33), respectively (Figure 4d and 4e), showing the near pure white-light emission via fluorescence and phosphorescence dual emission. To the best of our knowledge, the single coordination polymer without the introduction of guest emitters showing white-light emission is rare. These results indicate that coordination-induced crystallization provides an efficient way to develop white light materials.

To understand the origin and mechanism of the multiple long-lived peaks of compounds 1-3, temperature-dependent prompt and delayed emission are performed from 77 to 300 K. As shown in Figure 4f and S14, the emission intensity of compound 1 across the whole emission wavelength decreased gradually with the increasing temperature, even some emission peaks at long wavelength above 500 nm disappeared, confirmed that the long-lived emission peaks of compound 1 belongs to phosphorescence rather than thermally activated delayed fluorescence (TADF) [44,45]. The emission trace of compound 1 at 500 nm is very close to that of CzIP in the solution of chloroform at low temperature (Figure S17), suggesting the emission comes from the single molecule triplet state phosphorescence. The phosphorescence emission of these compounds has almost no change under the different excitation wavelengths, it can be reasonably speculated that the multiple emission did not be generated from different luminescent centers.[46,47] In addition, compared to the solid state

Preprints (www.preprints.org) | NOT PEER-REVIEWED | Posted: 27 April 2023 doi:10.20944/preprints202304.1017.v1

UV-Vis absorption of organic ligand powder, UV–vis absorption spectra of compounds 1-3 exhibited largely red-shifted bands (Figure S18 and S19), which can be attributed to the intramolecular and intermolecular charge transfer. Therefore, the origination of multiple phosphorescence bands could be tentatively assignable as the intermolecular charge transfer and the aggregation-induced emission of molecular cluster.[48,49] In addition, compound 3 only has faint phosphorescence with a short lifetime, it is mainly because that the dense aggregation with strong π–π interactions enhanced triplet–triplet annihilation and extended exciton diffusion, resulting in exciton quenching and the red shift of phosphorescence emission, and the photoluminescent behaviors is closer to the emission characteristic of the excimer (Figure 5a). [50,51] It should be pointed out that the phosphorescence property of compound 3 is different from the previous reported results, where the strong the π–π interactions can efficiently stable the excited triplet states, further prompt the generation of long-live room temperature phosphorescence. These results demonstrated that controlling the aggregate states of molecules can significantly modulate the singlet and triplet properties, further affect the phosphorescence performance.

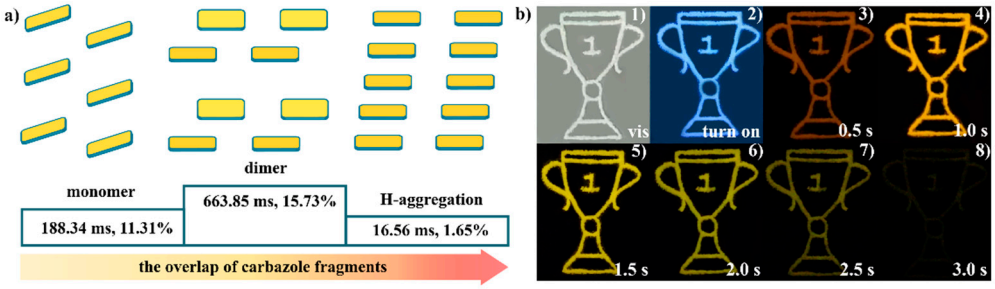

Figure 5. (a) The monomer-type aggregation of carbazole groups in compound 2, as well as dimer and H-aggregation in compounds 1 and 3; (b) the multiple-level anticounterfeiting of compound 1: the sample under natural light in Figure b1, under 365 nm UV sources in Fig.b2, the afterglow color was changed from orange to green to yellow green in Figure b3-b8.

Considering that the unique time-dependent long-lived room temperature phosphorescence of compound 1, the multiple-level anticounterfeiting was exploited. As shown in Figure 5b, A trophy label was prepared by using sample 1 powder. A "trophy"-like hole was made in a piece of cardboard with a thickness of 1 mm. The hole was filled with the fine powder of compound 1. Under 365 nm irradiation, the pattern exhibited the blue white emission. The UV light was switched off, the pattern emitted an orange afterglow for about 0.5 s, then a yellow afterglow, followed by a green emission could be observed by the naked eye. Compared to common anti-counterfeiting labels of the single afterglow materials, the tag generated by compound 1 is much more sophisticated, it is hard to be counterfeited, these results demonstrated the potential applications for multi-color display and anticounterfeiting.

3. Conclusions

In summary, we propose a coordination-induced approach to modulate the aggregation of CzIP, three compounds were synthesized. Compounds 1-3 with the different aggregated states of CzIP showed the different emission wavelengths, phosphorescent lifetimes and phosphorescent quantum yields. Interestingly, compound 1 showed the time-dependent multi-emission phosphorescence, the dynamic RTP behaviors may cause by the triplet excited states of the intramolecular electron coupling and the different aggregated states of CzIP. By comparing the phosphorescent performance synthetically, it reveals that the aggregate states are crucial to regulate the luminescent properties, importantly, we found that H-aggregation is not favorable to the generation of ultralong RTP in compound 3, this is not just like previous reports where H-aggregation can prompt the generation of ultralong RTP. Compounds 1 and 2 exhibited the white-light emission benefiting from fluorescence and phosphorescence dual emission. The photoluminescent CIE coordinates of compounds 1 and 2 were (0.33, 0.36) and (0.34, 0.33), respectively. In addition, the visible and high-level

anti-counterfeiting could be achieved by utilizing these dynamic phosphorescence materials. This work provides the good models to figure out the relationship between the accurate packing structures and the luminescent performance, opens an important approach for developing dynamic room temperature phosphorescence.

Author Contributions: H. Chen: conceptualization, measurements, K. Zhang and T. Li: data curation, formal analysis. X. L. Zhu: formal analysis, writing—original draft preparation and. H. R. Fu: writing—reviewing and editing, funding acquisition.

Data Availability Statement: The datasets supporting this article have been uploaded as the ESI.†

Acknowledgments: This work was supported by the Natural Science Foundation for Excellent Young Scholars of Henan Province (212300410061). The Scientific and Technological Support Project of Guizhou Province (Qian Ke He Zhi Cheng [2023] Yi Ban 262), Key scientific research projects of universities in Henan Province (21A150037).

Conflicts of Interest: There are no conflicts to declare.

References

1. Nidhankar, A.D; Gouda, G.; Wakchaure, V.C. and Babu, S.S.; Efficient metal-free organic room temperature phosphors. *Chem. Sci.*, **2021**, 12, 4216−4236. DOI: 10.1039/D1SC00446H
2. Hirata, S.; Recent advances in materials with room-temperature phosphorescence: photophysics for triplet exciton stabilization. *Adv. Opt. Mater*., **2017**, 5, 1700116. DOI: 10.1002/adom.201700116
3. Yan, X.; Peng, H.; Xiang, Y.; Wang, J.; Yu, L.; Tao, Y.; Li, H.; Huang, W and Chen, R.; Recent Advances on Host-Guest Material Systems toward Organic Room Temperature Phosphorescence. *Small*, **2022**, 18, 2104073. DOI: 10.1002/smll.202104073
4. Yang, X.; Dong, Y.; Ma, S.; Ren, J.; Li, N.; Lü, S.; Humidity-resistant organic room-temperature phosphorescence materials synthesized using catalyst-free click reaction. *Chem. Eng. J.*, **2023**, 462, 142198. DOI: 10.1016/j.cej.2023.142198
5. Kursunlu, A. N.; Porphyrin–Bodipy combination: synthesis, characterization and antenna effect, *RSC Adv.*, **2014**, 4, 47690-47696. DOI: 10.1039/C4RA09024A
6. Li, Y.; Li, Q.; Meng, S.; Qin, Y.; Cheng, D.; Gu, H.; Wang, Z.; Ye, Y.; Tan J.; Ultrabroad-band, white light emission from carbon dot-based materials with hybrid fluorescence/phosphorescence for single component white light-emitting diodes. *Chinese Chem. Lett.*, **2023**, 34, 107794. DOI: 10.1016/j.cclet.2022.107794
7. Kursunlu, A. N.; Guler, E.; The sensitivity and selectivity properties of a fluorescence sensor based on quinoline-Bodipy. *J. lumin*., **2014**, 145, 608-614. DOI: 10.1016/j.jlumin.2013.08.030
8. Ma, X. and Liu, Y.; Supramolecular Purely Organic Room-Temperature Phosphorescence. *Acc. Chem. Res.*, **2021**, 54, 3403–3414. DOI: 10.1021/acs.accounts.1c00336
9. Wang, H.; Yang, X.; Qin, J. and Ma, L.; Long-lived room temperature phosphorescence of organic–inorganic hybrid systems. Inorg. *Chem. Front*., **2021**, 8, 1942–1950. DOI: 10.1039/D0QI01508C
10. Li, D.; Lu, F.; Wang, J.; Hu, W.; Cao, X.; Ma, X. and Tian, H.; Amorphous Metal-Free Room-Temperature Phosphorescent Small Molecules with Multicolor Photoluminescence via a Host-Guest and Dual-Emission Strategy. *J. Am. Chem. Soc*., **2018**, 140, 1916–1923. DOI: 10.1021/jacs.7b12800
11. Zhao, W.; He, Z.; Jacky W. Y. Lam, Peng, Q.; Ma, H.; Shuai, Z.; Bai, G.; Hao, J. and Tang, B.; Rational Molecular Design for Achieving Persistent and Efficient Pure Organic Room-Temperature Phosphorescence. *Chem*, **2016**, 1, 592–602. DOI: 10.1016/j.chempr.2016.08.010
12. Garain, S.; Ansari, S.N.; Kongasseri, A.A.; Chandra G.B.; Pati, S.K. and George, S.J.; Room temperature charge-transfer phosphorescence from organic donor–acceptor Co-crystals. *Chem. Sci*., **2022**, 13, 10011–10019. DOI: 10.1039/D2SC03343G
13. Reineke, S.; Lindner, F.; Schwartz, G.; Seidler, N.; Walzer, K.; Lussem, B. and Leo, K.; White organic light-emitting diodes with fluorescent tube efficiency. *Nature*, **2009**, 459, 234–238. DOI: 10.1038/ncomms5016
14. Sinha, S.; Chowdhury, B.; Ghorai, U.K. and Ghosh, P.; Multitasking behaviour of a small organic compound: solid state bright white-light emission, mechanochromism and ratiometric sensing of Al(iii) and pyrophosphate. *Chem. Commun*., **2019**, 55, 5127–5130. DOI: 10.1039/C8CC10258A
15. Karmakar, A. and Li, J.; Luminescent MOFs (LMOFs): recent advancement towards a greener WLED technology. *Chem. Commun*., **2022**, 58, 10768–10788. DOI: 10.1039/D2CC03330E
16. Chen, Y.; Tang, K.; Chen, Y.; Shen, J.; Wu, Y.; Liu, S.; Lee, C.; Chen, C.; Lai, T.; Tung, S.; Jeng, R.; Hung, W.; Jiao, M.; Wu, C. and Chou, P.; Insight into the mechanism and outcoupling enhancement of excimer-associated white light generation. *Chem. Sci*., **2016**, 7, 3556–3563. DOI: 10.1039/C5SC04902D
17. Zhou, C.; Zhang, S.; Gao, Y.; Liu, H.; Shan, T.; Liang, X.; Yang, B. and Ma, Y.; Ternary Emission of Fluorescence and Dual Phosphorescence at Room Temperature: A Single-Molecule White Light Emitter

Based on Pure Organic Aza-Aromatic Material. *Adv. Funct. Mater.*, **2018**, 1802407. DOI: 10.1002/adfm.201802407

18. Xu, B.; Mu, Y.; Mao, Z.; Xie, Z.; Wu, H.; Zhang, Y.; Jin, C.; Chi, Z.; Liu, S.; Xu, J.; Wu, Y.; Lu, P.; Lien, A. and Bryce, M.; Achieving remarkable mechanochromism and white-light emission with thermally activated delayed fluorescence through the molecular heredity principle. *Chem. Sci.*, **2016**, 7, 2201–2206. DOI: 10.1039/c5sc04155d
19. Wang, H.; Wang, J.; Zhang, T.; Xie, Z.; Zhang, X.; Sun, H.; Xiao, Y.; Yu, T. and Huang, W.; Breaching Kasha's rule for dual emission: mechanisms, materials and applications. *J. Mater. Chem. C*, **2021**, 9, 10154–10172. DOI: 10.1039/D1TC01970H
20. Ono, T. and Hisaeda, Y.; Flexible-color tuning and white-light emission in three-, four-, and five-component host/guest co-crystals by charge-transfer emissions as well as effective energy transfers. *J. Mater. Chem. C*, **2019**, 7, 2829–2842. DOI: 10.1039/C8TC06165C
21. Li, Q. and Li, Z.; Molecular Packing: Another Key Point for the Performance of Organic and Polymeric Optoelectronic Materials. *Acc. Chem. Res.*, **2020**, 53, 962–973. DOI: 10.1021/acs.accounts.0c00060
22. Zhang, J.; Huang, X. and Chen, X.; Supramolecular isomerism in coordination polymers. *Chem. Soc. Rev.*, **2009**, 38, 2385–2396. DOI: 10.1039/B900317G
23. Dang,L.L.; Li, T.T.; Zhang, T.T.; Zhao, Y.; Chen, T.; Gao, X.; Ma, L.F. and Jin, G.X.; Highly selective synthesis and near-infrared photothermal conversion of metalla-Borromean ring and [2]catenane assemblies. *Chem. Sci.*, **2022**, 13, 5130–5140. DOI: 10.1039/D2SC00437B
24. Jiang, Y.; Zhang, K.; Zhou, M.; Gao, P. and Fu, H.; A fluorescence/phosphorescence dual-emitting metal-organic framework exhibiting two approaches for single-phase white-light emission. *J. Solid State Chem.*, **2021**, 304, 122563. DOI: 10.1016/j.jssc.2021.122563
25. Fu, H.R.; Jiang, Y.Y..; Luo, J.H.; Li, T.; A Robust Heterometallic Cd(II)/Ba(II)-Organic Framework with Exposed Amino Group and Active Sites Exhibiting Excellent CO_2/CH_4 and C_2H_2/CH_4 Separation. *Chin. J. Struct. Chem.*, **2022**, 41, 2203287–2203292. DOI: 10.14102/j.cnki.0254-5861.2011-3340
26. Yuan, J.; Dong, J.; Lei, S. and Hu, W.; Long afterglow MOFs: a frontier study on synthesis and applications. *Mater. Chem. Front.*, **2021**, 5, 6824–6849. DOI: 10.1039/D1QM00689D
27. Jiang, Y.; Liu, H.; Li, T.; Zhang, K.; Gao, P.; M. Zhou, Zhang L. and Fu, H.; Coordination-Induced Approach of a Carbazole-Based Molecule to Modulate Packing Modes for Ultralong Room-Temperature Phosphorescence. *Cryst. Growth Des.*, **2022**, 22, 2725–2732. DOI: 10.1021/acs.cgd.2c00113
28. Zhou, H.; Han, J.; Cuan, J. and Zhou, Y.; Responsive luminescent MOF materials for advanced anticounterfeiting. *Chem. Eng. J.*, **2022**, 431, 134170. DOI: 10.1016/j.cej.2021.134170
29. Wen, Y.; Liu, H.; Zhang, S.; Gao, Y.; Yan, Y. and Yang, B.; One-dimensional π–π stacking induces highly efficient pure organic room-temperature phosphorescence and ternary-emission single-molecule white light. *J. Mater. Chem. C*, **2019**, 7, 12502–12508. DOI: 10.1039/C9TC04580E
30. Yang, Y.; Yang, X.; Fang, X.; Wang, K. and Yan, D.; Reversible Mechanochromic Delayed Fluorescence in 2D Metal-Organic Micro/Nanosheets: Switching Singlet-Triplet States through Transformation between Exciplex and Excimer. *Adv. Sci.*, **2018**, 5, 1801187. DOI: 10.1002/advs.201801187
31. Wang, Z.; Zhu, C.; Wei, Z.; Fan, Y. and Pan, M.; Breathing-Ignited Long Persistent Luminescence in a Resilient Metal–Organic Framework. *Chem. Mater.*, **2020**, 32, 841–848. DOI: 10.1021/acs.chemmater.9b04440
32. Liu, J.; Chen, Z.; Hu, J.; Sun, H.; Liu, Y.; Liu, Z.; Li, J.; Time-resolved color-changing long-afterglow for security systems based on metal–organic hybrids. *Inorg. Chem. Front.*, **2022**, 9, 584–591. DOI: 10.1039/d1qi01435h
33. Wang, Z.; Zhu, C. Y.; Mo, J. T.; Xu, X. Y.; Ruan, J.; Pan, M.; Su, C. Y.; Multi-mode Color-tunable Long Persistent Luminescence in Single Component Coordination Polymers. *Angew Chem., Int Ed*, **2021**, 60, 2526–2533. DOI: 10.1002/anie.202012831
34. Shi, Y.; Ma, H.; Sun, Z.; Zhao, W.; Sun, G.; Peng, Q.; Optimal Dihedral Angle in Twisted Donor–Acceptor Organic Emitters for Maximized Thermally Activated Delayed Fluorescence. *Angew. Chem., Int. Ed.*, **2022**, 61, e202213463. DOI: 10.1002/anie.202213463
35. Qian,C.; Ma, Z.; Fu, X.; Zhang, X.; Li, Z.; Jin, H.; Chen, M.; Jiang, H.; Jia X. and Ma, Z.; More than Carbazole Derivatives Activate Room Temperature Ultralong Organic Phosphorescence of Benzoindole Derivatives. *Adv. Mater.*, **2022**, 34, 2200544. DOI: 10.1002/adma.202200544
36. Ling, K.; Shi, H.; Wang, H.; Fu, L.; Lv, A.; Huang, K.; Ye, W.; Gu, M.; Ma, C.; Yao, X.; Jia, W.; Zhi, J.; Yao, W.; An, Z.; Ma, H. and Huang, W.; Prolonging Ultralong Organic Phosphorescence Lifetime to 2.5 s through Confining Rotation in Molecular Rotor. *Adv. Opt. Mater.*, **2019**, 7, 1800820. DOI: 10.1002/adom.201800820
37. Zhou,M.; Gao, P.; Jiang, Y.; Zhou, Y.; Wu, J.; Zhu, X. and Fu, H.; Multiemission tunability with ultralong and time–dependent room-temperature phosphorescence from isophthalic acid-decorated carbazole by coordination–induced crystallization. *Dyes Pigm.*, **2021**, 195, 109715. DOI: 10.1016/j.dyepig.2021.109715
38. Sheldrick,G.M.; Crystal structure refinement with SHELXL. *Acta Crystallogr. C*, **2015**, 71, 3–8. DOI: 10.1107/S2053229614024218

39. Bourhis,L.J.; Dolomanov, O.V.; Gildea, R.J.; Howard, J.A.K. and Puschmann, H.; SHELXT-integrated space-group and crystal-structure determination. *Acta Cryst.* **2015**. *A71, 3-8*. DOI: 10.1107/S2053273314026370
40. Janiak,C.; A critical account on π–π stacking in metal complexes with aromatic nitrogen-containing ligands. *J. Chem. Soc., Dalton Trans.*, **2000**, 3885–3896. DOI: 10.1039/B003010O
41. Jena, S.; Munthasir, A.T.M. and Thilagar, P.; Ultralong room temperature phosphorescence and ultraviolet fluorescence from simple triarylphosphine oxides. *J. Mater. Chem. C*, **2022**, 10, 9124–9131. DOI: 10.1039/D2TC01318E
42. Liu, H.; Zhang, K.; Gao, P.; Luo, J.; Jiang, Y.; Zhou, M.; Li, T.; Zhu, X. and Fu, H.; Realization of Single-Phase White-Light-Emitting Materials with Time-Evolution Ultralong Room-Temperature Phosphorescence by Coordination Assemblies. *Inorg. Chem.*, **2022**, 61, 1636−1643. DOI: 10.1021/acs.inorgchem.1c03461
43. Liu, Y.; Ma, Z.; Liu, J.; Chen, M.; Ma, Z. and Jia, X.; Robust White-Light Emitting and Multi-Responsive Luminescence of a Dual-Mode Phosphorescence Molecule. *Adv. Opt. Mater.*, **2021**, 9, 2001685. DOI: 10.1002/adom.202001685
44. Wei, Q.; Kleine, P.; Karpov, Y.; Qiu, X.; Komber, H.; Sahre, K.; Kiriy, A.; Lygaitis, R.; Lenk, S.; Reineke, S.; Voit, B.; Conjugation-Induced Thermally Activated Delayed Fluorescence (TADF): From Conventional Non-TADF Units to TADF-Active Polymers. *Adv. Funct. Mater.*, **2017**, 27, 1605051. DOI: 10.1002/adfm.201605051
45. Gužauskas, M.; Narbutaitis, E.; Volyniuk, D.; Baryshnikov, G.; Minaev, B.; Ågren, H.; Chao, Y.; Chang, C.; Rutkis, M.; Grazulevicius, J.; Polymorph acceptor-based triads with photoinduced TADF for UV sensing. *Chem. Eng. J.*, **2021**, 425, 131549. DOI: 10.1016/j.cej.2021.131549
46. Dou,X.; Zhu, T.; Wang, Z.; Sun, W.; Lai, Y.; Sui, K.; Tan, Y.; Zhang, Y. and Yuan, W.; Color-Tunable, Excitation-Dependent, and Time-Dependent Afterglows from Pure Organic Amorphous Polymers. Adv. *Mater.*, **2020**, 32, 2004768. DOI: 10.1002/adma.202004768
47. Li, H.; Gu, J.; Wang, Z.; Wang, J.; He, F.; Li, P.; Tao, Y.; Li, H.; Xie, G.; Huang, W.; Zheng, C. and Chen, R.; Single-component color-tunable circularly polarized organic afterglow through chiral clusterization. *Nat. Commun.*, **2022**, 13, 429. DOI: 10.1038/s41467-022-28070-9
48. Chen, J.; Yu, T.; Ubba, E.; Xie, Z.; Yang, Z.; Zhang, Y.; Liu, S.; Xu, J.; Aldred, M.P. and Chi, Z.; Achieving Dual-Emissive and Time-Dependent Evolutive Organic Afterglow by Bridging Molecules with Weak Intermolecular Hydrogen Bonding. *Adv. Opt. Mater.* **2019**, 7, 1801593. DOI: 10.1002/adom.201801593
49. Forni, A.; Lucenti, E.; Botta, C. and Cariati, E.; Metal free room temperature phosphorescence from molecular self-interactions in the solid state. *J. Mater. Chem. C*, **2018**, 6, 4603–4626. DOI: 10.1039/C8TC01007B
50. Hamzehpoor, E. and Perepichka, D.F.; Crystal Engineering of Room Temperature Phosphorescence in Organic Solids. *Angew. Chem. Int. Ed.*, **2020**, 59, 9977–9981. DOI: 10.1002/anie.201913393
51. Wang,Y.; Yang, J.; Tian, Y.; Fang, M.; Liao, Q.; Wang, L.; Hu, W.; Tang, B. and Li, Z.; Persistent organic room temperature phosphorescence: what is the role of molecular dimers? *Chem. Sci.*, **2020**, 11, 833−838. DOI: 10.1039/C9SC04632A